

# Crack analysis of micro-textured cutting tool

Arata Pradhan, Kashfull Orra\*

Indian Institute of Information Technology Design and Manufacturing Kancheepuram, Chennai, India

Presented in International Conference on Precision, Micro, Meso and Nano Engineering (COPEN - 12: 2022)

December 8 - 10, 2022 IIT Kanpur, India

---

## ABSTRACT

---

### KEYWORDS

Extended Finite Element,  
Crack Analysis,  
Textured Tool,  
Machining.

*Texturing on the tool rake surface is one type of crack induced on the tool surface by surface-texturing technologies that have the potential to produce micro-cracks. The surface grooves may act as notches that will lead to stress concentration and eventually initiate the crack or propagate the induced cracks. This work has attempted to study crack initiation and propagation, particularly on the textured tool with V-shaped cross-section grooves provided to the textured tool model. To investigate this, the extended finite element method is used to govern the initiation and propagation of fractures in the tool domain. Results obtained from the study suggested that textured tools are substantially more prone to cracking than untextured tools. Its critical displacement value for the untextured tools is about 55 % more compared to the textured tool. Findings led to the conclusion that the depth, width, and pitch of the grooves have a direct impact on tool cracking.*

---

## 1. Introduction

Texturing on the cutting tool face is recently used in industries to improve the machining performance and cutting tool life in a variety of ways, including entrapping wear debris, providing lubricants, increasing shear angle, chip breakage, anti-adhesion, and acting as wear resistance that helps in reducing chip curl radius, work hardening and oxidation degree of machined surface (Fan et al., 2021). Table 1 shows results in the percentage reduction of responses depending on the experimental setup, machining condition, and texture geometry. It has been observed that there is a significant reduction in machining performance by textured tools when compared to standard untextured tools. The primary and secondary shear planes are reduced during chip formation due to the presence of texture on the cutting tool face and associated tribological changes at the tool-chip interface. As a result, machining forces and coefficient of friction are lowered, leading to lower power consumption, which can be a step toward sustainability (Bertolete et al., 2018). Additionally, this textured cutting tool reduced the actual tool-chip contact area. Therefore, the coefficient of friction and cutting temperature at the tool-chip interface was usually

lower with textured tools. Moreover, the micro-textures entrap air, which acts as a self-lubricant and further reduces the temperature, also micro-textures on the rake surface behaves like artificial fins transferring the heat to the air (Orra & Choudhury, 2018).

However, texture fabrication techniques generate micro-cracks as a by-product. Hazzan et al. (2022) observed that the laser caused cracking, thermal shock, porosity, and other surface damage to tungsten carbide. The WC grains thermal stress and phase transition cause surface cracking at the bottom of the grooves (Chu et al., 2021).

Therefore, from all the research work done as mentioned above in the literature, it can be concluded that the studies have concentrated on improving or optimizing texture design parameters to improve machining performance. There has been no research into damage analysis associated with the micro-textured tool and optimizing texture design parameters to reduce the effect of crack initiation and propagation. The present objective of this research paper is to investigate the nature of crack initiation and propagation on textured and untextured tools using the extended finite element method, a comprehensive parametric study comparing textured and untextured tools has been carried out. In this, texturing methods have the tendency to induce micro-cracks, which could be considered as

---

\*Corresponding author E-mail: orra@iitdm.ac.in

<https://doi.org/10.58368/MTT.22.4.2023.26-31>

**Table 1**  
Literature survey.

Reference	Coefficient of friction	Cutting force	Cutting temperature	Roughness	Flank wear
Bertolete et al. (2018)	-	20%	-	46%	-
Ahmed et al. (2020)	24%	58%	-	68%	78%
Qian et al. (2020)	-	19%	-	39%	-
Sivaiah et al. (2019)	-	-	25%	42%	40%
Siddiqui et al. (2021)	-	-	40%	-	35%

crack initiation. Micro-cracks can also form and propagate during the machining process as well, because of the cutting tools deflection due to cutting loads acting on the tooltip.

**2. FEM Analysis and Modelling**

The extended finite element method (XFEM) solves the crack propagation problem in less time and effort respectively. It is suitable to predict crack initiation, as well as determine and trace their propagation along an arbitrary direction, and it is a solution-dependent path without re-meshing. This is because XFEM allows the presence of discontinuities in an element by enriching degrees of freedom with special displacement functions. In this current study V-shaped cross-section grooves are created in the XFEM textured tool model for the analysis of crack propagation with the following design parameters, width 60 μm – 120 μm; depth 30 μm – 90 μm and pitch 150 μm – 250 μm. Figure 1 shows the cutting tool geometrical model for untextured (UT) and surface textured (ST) tools respectively.

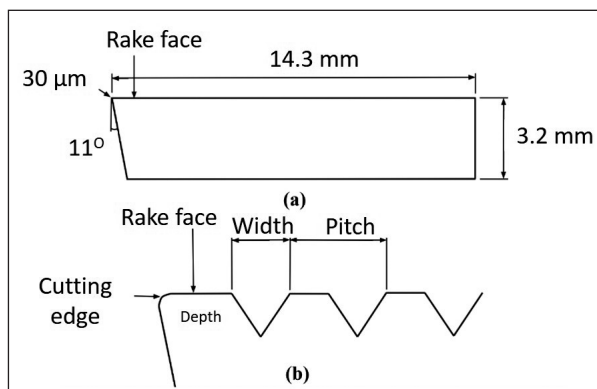


**Fig. 1.** Tool model: (a) Untextured (UT), (b) Surface textured (ST).

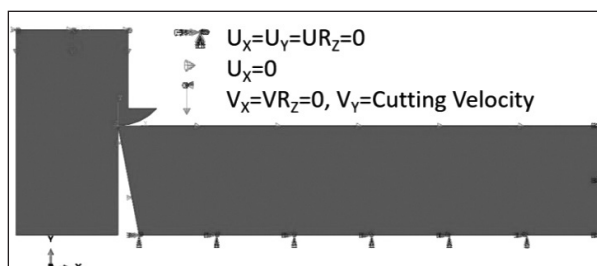


**Fig. 2.** Cutting tool and workpiece with boundary condition.

To conduct numerical simulations in the current research paper, the workpiece is considered rigid while the machining action is static. The boundary conditions given to the workpiece and cutting tool are shown in Fig. 2. The physical properties of tungsten carbide are taken from the literature (Ashby, 2011). The fracture energy of the tungsten carbide is calculated by Eq. (1) and is given below.

$$G_I = \frac{K_{IC}^2}{E} \dots\dots\dots(1)$$

Where,  $G_I$  is fracture energy  $K_{IC}$  is fracture toughness and  $E$  is young's modulus, which yields fracture energy of 12.74 J/m<sup>2</sup> for tungsten carbide, which has been used in the numerical analysis for both normal and shear modes, assuming they are equal.

The cutting tool has been modeled as a linearly elastic solid. For traction-separation laws, stress-based criteria (Maximum principal stress criterion) for damage initiation and energy-based criteria for damage evolution are adopted in ABAQUS for solving numerically. According to the maximum principal stress criterion (Eq. (2)), cracks for brittle tungsten carbide begin when the tool's maximum principal stress (yield stress) reaches the critical value of about 5.09 GPa. Alternatively, when  $f = 1$ , the damage is assumed to initiate. Damage evolution rules based on energy and linear softening were then provided using the B-K formulation (Benzeggagh and Kenane, 1996) given in Eq. (3) to calculate the effective energy release rate.

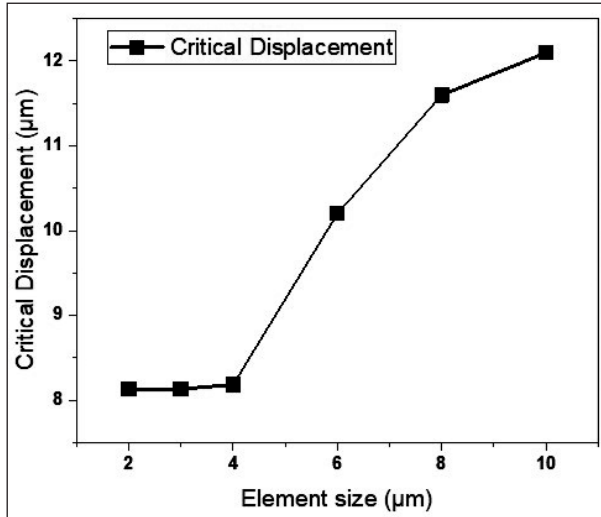


Fig. 3. Mesh sensitivity analysis.

$$f = \left\{ \frac{\sigma_{max}}{\sigma_{max}^0} \right\} \dots\dots\dots(2)$$

$$G_{equiv\ c} = G_{IC} + (G_{IIC} - G_{IC}) \left( \frac{G_I + G_{II}}{G_I + G_{II} + G_{III}} \right)^\eta \dots\dots\dots(3)$$

Where  $\sigma_{max}$  is maximum principal stress,  $\sigma_{max}^0$  is the maximum allowed principal stress,  $G_{equiv\ c}$  is the total mixed-mode fracture energy,  $G_I$  is the strain energy release rate in the normal direction,  $G_{II}$  and  $G_{III}$  is strain energy rates in two directions,  $G_{IC}$  and  $G_{IIC}$  is normal fracture energy and shear fracture energy respectively. The factor  $\eta$  is the B-K material parameter.

2.1. Mesh strategies

The mesh size has a significant impact on the simulation results in terms of accuracy and the amount of CPU time required for each time step. Thus, a study area near the tooltip has been created for the analysis to reduce the computing time. The study area zone at the tool chip interface has a higher mesh density than the rest of the region, as a result, the number of elements has been significantly reduced. Moreover, mesh sensitivity analysis has been carried out by mesh refinement process by reducing element size in the studied zone area until the obtained solution is no longer dependent on mesh element size. Therefore, the element size has been reduced in the study zone area from 8 µm to 1 µm. Thereafter, the displacement done by the workpiece for initiating the crack is then compared. Thus when the size of the adopted elements is between 4 µm and 2 µm, the critical displacement trend stabilized, shown in Fig. 3.

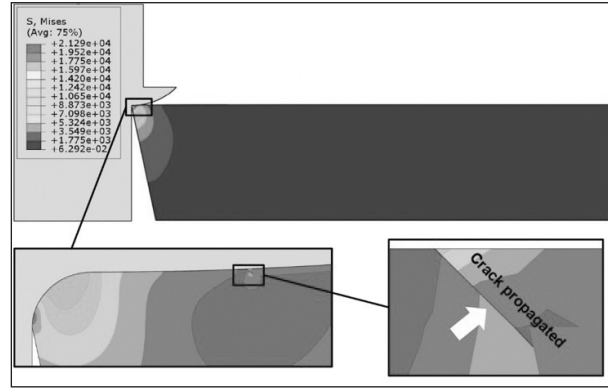


Fig. 4. Crack propagated in the untextured tool at a critical displacement of 20 µm.

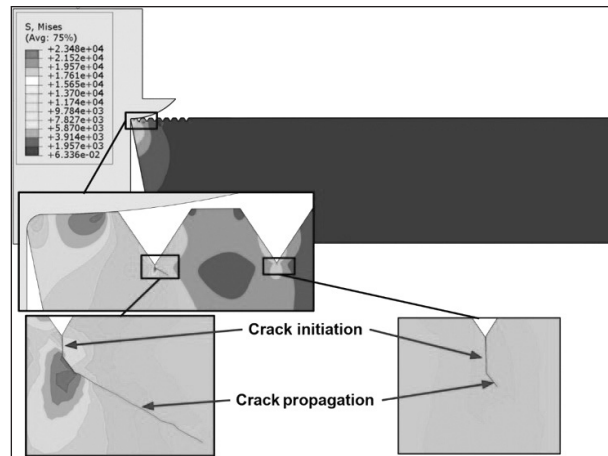


Fig. 5. Crack propagated in the surface textured tool at a critical displacement of 20 µm with crack initiation provided.

3. Results and Discussion

3.1. Crack initiation and propagation stage for textured and untextured tool

The analysis has been carried out using two different tools. One is a surface textured tool (ST) with V-cross section grooves, while the other is an untextured tool (UT). The edge radius of both tools is about 25 µm and the rake angle is zero (0°). The workpiece velocity is used to model the cutting speed with a value of 120 m/min, and the dimensions considered for textured tool grooves are depth and width of about 90 µm each and a pitch of about 150 µm. Figures 4 and 5 show the nature of crack initiation and propagation for UT and ST tools respectively after the initiation step, where the entire tool area has been assigned as XFEM. Further to analyse crack propagation in the textured tool, additionally crack location has been provided for all grooves for textured tools. Thus when the principal stress

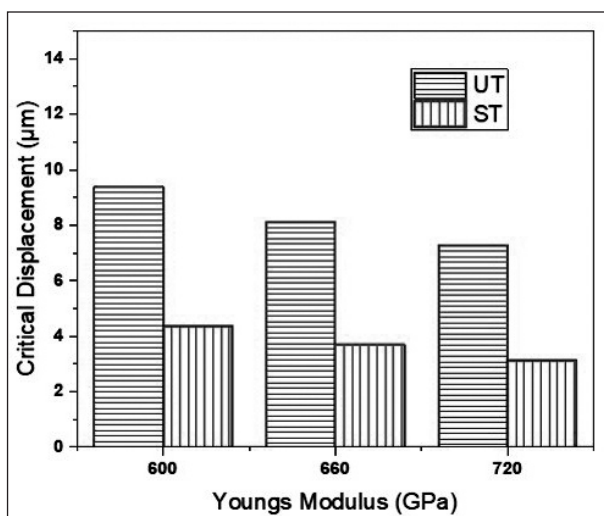


Fig. 6. Influence of texturing, untextured (UT), and surface textured (ST) on crack initiation.

reaches its maximum value of about 5.09 GPa, fracture initiation occurs at the bottom of the grooves. This is because these micro textures on the tool act as V-notch, hence increasing the probability of failure modes. This V-notch usually acts as a singular stress concentrator, and this kind of stress singularity leads to fracture and crack propagation.

### 3.2. Influence of texturing on crack initiation

Figure 6 shows the critical displacement, required for crack initiation, and varies as a function of stiffness for textured and untextured cutting tools. The critical displacement decreases and the average critical displacement for untextured tools are about 55% larger than for surface textured tools. This signifies that the textured tool is prone to crack initiation and propagation, this may be because the micro-grooves weaken the tool strength and propagation of micro-cracks are unavoidable. This may be due to the techniques used to fabricate the textures, such as LST (Laser surface texturing) and EDM (Electric discharge machining), which cause the formation of micro-cracks due to irregularities in thermal expansion rate occurs during processing Hazzan et al. (2022). The cracks in tungsten carbide are mainly due to the plastic deformation of the metal binder. The dislocations and stacking faults in WC grains also contribute to the plastic deformation of the cemented carbide (Ashby, 2011). Thus, textured tools are more prone to cause a crack, to reduce cracks, further investigations are needed by changing the texture design parameters without distorting the benefits of textured tools is discussed in the subsequent sections.

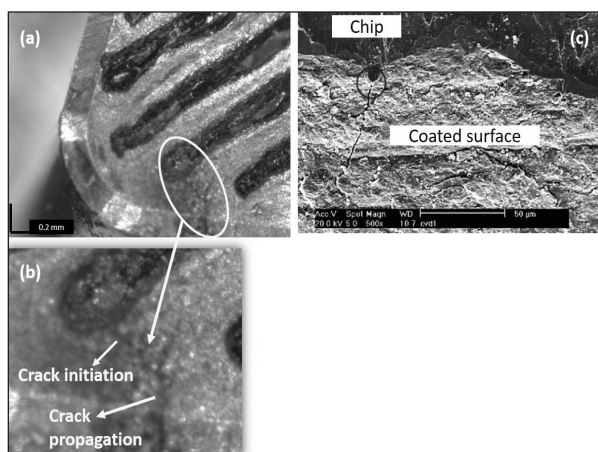


Fig. 7. (a) Micro-cracks representation; (b) magnified image of crack initiation and propagation; (c) cracking at the interface at  $V = 100$  m/min,  $f = 0.15$  mm/rev and  $d = 2$  mm (Nouari and Ginting, 2006).

### 3.3. Influence of texture geometry on crack initiation and propagation

In this section, the effect of texture design parameters on crack initiation and propagation has been analyzed. Varying geometrical parameters for texture design were used for the numerical analysis, such as width, depth, and pitch of about  $60 \mu\text{m} - 120 \mu\text{m}$ ,  $30 \mu\text{m} - 90 \mu\text{m}$  and  $150 - 200 \mu\text{m}$  respectively. In addition, the constant rake angle and radius of the cutting edge are set to  $0^\circ$  and  $25 \mu\text{m}$  respectively. The simulation results obtained for critical displacement values to initiate and propagate crack to investigate the effect of texture design parameters vary in the range of  $2.5486 \mu\text{m} - 8.0238 \mu\text{m}$  and  $7.1276 \mu\text{m} - 16.248 \mu\text{m}$  respectively. Here grooves on the tool rake face are assumed to be a notch. During machining when the tool and workpiece are in contact, the notch causes a stress concentration and increases the transition temperature due to the high strain rate increasing the stress for dislocation. This may lead to fatigue crack initiation and growth due to slip and twinning along the grain boundary. Figure 7 shows the pictorial representation of the micro-cracks at the cutting edges occur due to mechanical load acting at the tool-chip interface.

### 3.4. Rake angle's influence on crack initiation

The geometry of the cutting tool, i.e., rake angle, clearance angle, and cutting edge radius, has a direct impact on the machinability and the machined product's quality, which necessitates an investigation of this prospect. Thus, analysis has been done to investigate the influence of rake angle on crack initiation by varying rake angle.

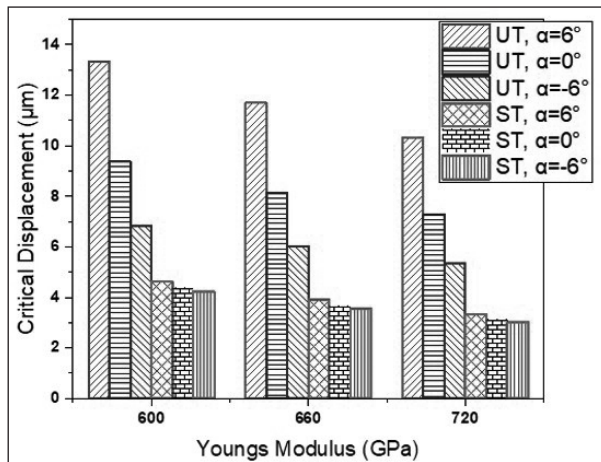


Fig. 8. Effect of rake angle ( $\alpha$ ) at  $-6^\circ$ ,  $0^\circ$ , and  $6^\circ$  on crack initiation.

Figure 8 shows that when the rake angle changes from negative to positive, the displacement value increases in both untextured (UT) and surface textured (ST) tools, which implies that the tool's tendency to initiate crack reduces. This can be explained by the fact that due to a decrease in friction force and true surface energy there is a decrease in cutting forces. Moreover, a cutting tool with a positive rake angle produces lower cutting force, tool wear, and heat generation than cutting tools with a negative rake angle. This may be due to the negative rake angle resulting in a larger contact area and a higher chip volume. A similar result was observed in the numerical analysis given by Bounif et al. (2021). They found that using cutting tools with positive rake angles reduces the probability of crack initiation and propagation in the coating when compared to neutral and negative rake angles.

#### 4. Conclusions

In this study, XFEM is used to govern the initiation and propagation of fractures in the tool domain, and the critical displacement in terms of critical fracture stress is used to analyse the results. The sole goal of this numerical analysis is to show textured tools tend to crack initiation and propagation and to identify the texture geometry responsible for crack initiation and propagation, which researchers may further consider when fabricating textured tools.

First, parametric studies have been done to compare untextured tools and textured tools, the results show that:

- The critical displacement value for the untextured tools is found to be about 55%

more compared to the textured tool. So, it has been concluded that textured tools are much more prone to cracking.

Second, using variance, the effect of texture design parameters on fracture initiation and propagation was investigated. The study's findings lead to the conclusion that

- The depth and width of the groove have a direct impact on tool cracking. The tool is more prone to cracking due to the deep groove depth and narrow groove width.
- The pitch, on the other hand, is less likely to affect the tool cracking.

A further parametric study found that

- The tool's high rigidity and high rake angle prevent it from cracking in both textured and untextured environments. Hence, experimentation work in the future needs investigation to support and reveal characteristics of these texture design parameters on crack initiation and propagation. Overall the current study's findings can be used by researchers and the cutting tool industry when fabricating textured tools.

#### Acknowledgments

The authors would like to thank the Department of Mechanical Engineering and Centre for Smart Manufacturing, IITDM Kancheepuram, Chennai, India for the support towards the study. This research did not receive any specific grant from funding agencies in the public, commercial, or not-for-profit sectors.

#### Reference

Ahmed, Y. S., Paiva, J.M., Arif, A.F.M., Amorim, F.L., Torres, R.D., & Veldhuis, S.C. (2020). The effect of laser micro-scale textured tools on the tool-chip interface performance and surface integrity during austenitic stainless-steel turning. *Applied Surface Science*, 510, 145455. <https://doi.org/10.1016/j.apsusc.2020.145455>

Ashby, M.F. (2011). *Material selection in mechanical design*. 4th ed. USA: Elsevier.

Benzeggagh, M. L., & Kenane, M. (1996). Measurement of mixed-mode delamination fracture toughness of unidirectional glass/epoxy composites with mixed-mode bending apparatus. *Composites Science and Technology*, 56, 439-449. [https://doi.org/10.1016/0266-3538\(96\)00005-X](https://doi.org/10.1016/0266-3538(96)00005-X)

Bertolete, M., Barbosa, P. A., Machado, A. R., Samad, R. E., Vieira Jr., N. D., Vilar, R., & Rossi, W. D. (2018). Effects of texturing the rake surfaces of cemented tungsten carbide tools by ultrashort laser pulses in machining of martensitic stainless steel. *International Journal of Advanced Manufacturing Technology*, 98, 2653-2664. <https://doi.org/10.1007/s00170-018-2407-x>

Bounif, K., Abbadi, M., Nouari, M., & Selvam, R. (2021). A numerical approach for crack-induced damage in tungsten carbide cutting tools during machining. *Engineering Failure Analysis*, 128, 105617. <https://doi.org/10.1016/j.engfailanal.2021.105617>

Chu, C., Zhang, Q., Zhuo, H., Zhang, Z., Zhu, Y., & Fu, Y. (2021). Investigation on the ablation behavior of cemented tungsten carbide by a nanosecond UV laser. *Journal of Manufacturing Processes*, 71, 461-471. <https://doi.org/10.1016/j.jmapro.2021.09.038>

Fan, L., Deng, Z., Gao, X., & He, Y. (2021). Cutting performance of micro-textured PCBN tool. *Nanotechnology and Precision Engineering*, 4, 023004. <https://doi.org/10.1063/1.50004372>

Hazzan, K. E., Pacella, M., & See, T. L. (2022). Understanding the surface integrity of laser surface engineered tungsten carbide. *International Journal of Advanced Manufacturing Technology*, 118, 1141-1163. <https://doi.org/10.1007/s00170-021-07885-8>

Nouari, M., & Ginting, A. (2006). Wear characteristics and performance of multi-layer CVD-coated alloyed carbide tool in dry end milling of titanium alloy. *Surface & Coatings Technology*, 200, 5663-5676. <https://doi.org/10.1016/j.surfcoat.2005.07.063>

Orra, K., & Choudhury, S. K. (2018). Tribological aspects of various geometrically shaped micro-textures on cutting insert to improve tool life in hard turning process. *Journal of Manufacturing Processes*, 31, 502-513. <https://doi.org/10.1016/j.jmapro.2017.12.005>

Qian, X., Duan, X., & Zou, J. (2020). Effects of different tool microstructures on the precision turning of titanium alloy TC21. *International Journal of Advanced Manufacturing Technology*, 106, 5519-5526. <https://doi.org/10.1007/s00170-020-05009-2>

Siddiqui, T. U., & Singh, S. K. (2021). Design, fabrication and characterization of a self-lubricated textured tool in dry machining.

*Materials Today: Proceedings*. 41, 863-869. <https://doi.org/10.1016/j.matpr.2020.09.259>

Sivaiah, P. (2019). Evaluation of hybrid textured tool performance under minimum quantity lubrication while turning of AISI 304 steel, *Journal of the Brazilian Society of Mechanical Sciences and Engineering*, 41, 1-8. <https://doi.org/10.1007/s40430-019-2069-0>



**Arata Pradhan** holds a master's degree in Mechanical Systems Design from the Indian Institute of Information Technology Design and Manufacturing Kancheepuram, Chennai. He graduated from Biju

Patnaik University of Technology, Odisha with a bachelor's degree in Mechanical Engineering. His Master thesis work was on numerical analysis on textured tools. He has worked as a Data Analyst in Dynata Hyderabad, India. His research interest is in solid mechanics and machining and currently pursuing Ph.D. at IIT Palakkad. (E-mail: aratapradhan20@gmail.com)



**Dr. Kashfull Orra** an Assistant Professor in the Department of Mechanical Engineering, Indian Institute of Information Technology Design and Manufacturing Kancheepuram, Chennai, India. He

earned Ph.D degree in Manufacturing Science from Indian Institute of Technology Kanpur in the year 2019. His area of interest and research is online monitoring and controlling machine tool vibration, and improving the process performance using closed-loop adaptive control systems, as well as he is working on composite materials. He has published papers at reputed International and national conferences.